Materials Horizons

Accepted Manuscript

ROYAL SOCIETY OF CHEMISTRY

rsc.li/materials-horizons

Conceptual Insights

Due to its high capacity for lithium storage, sulfur is a leading candidate to succeed the metal-oxide cathode materials that are currently used in lithium-ion batteries. The biggest challenge for the further development of lithium-sulfur batteries is the solubility and mobility of lithium polysulfide species, which results in poor coulombic efficiency and cycle life. In this work we encapsulate lithium-polysulfides in a porous silica network using sol-gel chemistry. The resulting material is a solid cathode that reversibly stores lithium. In order to limit water formation during gelation we use a novel processing route where a non-hydrolytic sol is dehydrated using heat and vacuum. The ability to encapsulate water-sensitive and redox-active materials by sol-gel chemistry should be applicable to researchers outside of the battery field.

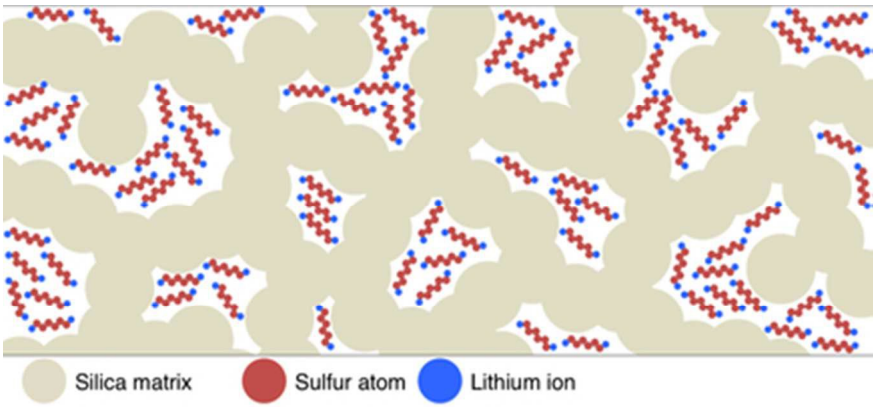

36x16mm (300 x 300 DPI)

Sol-gel encapsulated lithium polysulfide catholyte and its application in lithium-sulfur batteries

Leland C. Smith[a*], Peter Malati[ab], Jonathan Fang[ac], Wade Richardson[ad], David Ashby[a], Chun Han Lai[a] and Bruce S. Dunn[a]

[a] Department of Materials Science and Engineering, University of California at Los Angeles, Los Angeles, CA 90095, USA
[b] Teledyne Scientific Company, 1049 Camino Dos Rios, Thousand Oaks, CA, USA
[c] TLC Biopharmaceuticals, Inc., 432 North Canal Street, Suite #20, South San Francisco, CA 94080
[d] StemBios Technologies, Inc., 2530 Corporate Place, STE A112 Monterey Park, CA 91754

* corresponding author

† Electronic supplementary information (ESI) available:

Abstract

Lithium polysulfides are the active cathode species in lithium-sulfur batteries. In this work non-hydrolytic sol-gel chemistry is tuned to create a sol that successfully encapsulates lithium polysulfide solutions, forming a solid polysulfide gel. The chemistry of the polysulfide gel is studied using Fourier transform infrared and Raman spectroscopies, which confirm the presence of active lithium polysulfides. This polysulfide gel is incorporated into a solid state lithium sulfur battery and cycled galvanostatically. Electrochemical impedance spectroscopy confirms that the gel has very similar electrochemical properties to the lithium polysulfide solutions from which it was prepared. Discharge capacities as high as 1 mAh/cm^2 are obtained for a polysulfide gel cathode that is 1 mm thick.

Introduction

The performance of modern lithium-ion batteries is primarily limited by the capacity of transition metal oxide cathodes, which at ≤ 150 mAh/g is less than half that of graphite anodes.[1] Sulfur is a promising alternative cathode material, with a theoretical lithium capacity of 1675 mAh/g for complete reduction to Li_2S.[2] Unlike the topotactic lithium insertion reactions that occur in transition metal oxide cathodes, lithium reacts with sulfur through the formation of polysulfide species with different sulfur chain lengths (n) giving a general formula of Li_2S_n.

While promising, the Li-S system is beset by a number of problems. Sulfur is a poor electrical conductor and requires the addition of conductive additives. The lower order polysulfides ($n < 3$) are generally insoluble in the aprotic solvents (e.g. tetrahydrofuran, dioxolane) used in electrolytes for lithium-sulfur batteries (LSB), which can lead to irreversible capacity loss and low cycle life. Because the longer ($n \geq 3$) polysulfide species are soluble in these solvents, they have a tendency to diffuse to the lithium electrode and react directly thereby circumventing the external circuit and acting as an internal short.[3] This effect is often referred to as the shuttle mechanism.

Various groups have worked to improve the cycle life and efficiency of LSB either by trapping the sulfur species in the cathode, passivating the lithium anode surface, or both. A typical entrapment method involves forming a composite cathode by coating sulfur particles with polymers such as polyethylene oxide and various forms of carbon including graphene.[4] Carbon-confinement has also been applied to a related cathode material, selenium.[5] In addition, researchers have used oxides (silica and titania) as resevoirs to help trap the soluble polysulfides.[6]

Passivation methods have also been successful in inhibiting the shuttle mechanism and improving the cycle life of LSB. Yang et al. used a fully liquid polysulfide cathode in a flow battery configuration, with $LiNO_3$ as an additive used to passivate the lithium metal.[7,8] Demir-Cakan et al. reacted sulfur powder directly on the surface of lithium metal, forming a passivating polysulfide layer in-situ.[9] In another approach, Lin et al. synthesized lithium polysulfidophosphates, sulfur containing materials with modest (10^{-4} to 10^{-6} S/cm) lithium-ion conductivity, as fully solid-state sulfur cathodes.[10]

In this work we develop a new entrapment method for LSB. The present paper applies sol-gel chemistry to solutions of lithium-polysulfides and leads to a novel material, a polysulfide gel

(PG), which is electrochemically active. Using the PG as a cathode, we fabricate a LSB using a lithium metal anode and molybdenum current collector.

One unique feature of the sol-gel process is its ability to produce materials in which a continuous liquid phase is confined within an interconnected porous network composed of the sol-gel derived oxide. By tailoring the nanoscale morphology of the oxide, typically silica, the resulting gels are macroscopically rigid and yet exhibit properties which are characteristic of the liquid. Some of the first examples of this approach are the encapsulation of organic liquid electrolytes producing gels with conducitivity ~ 10^{-3} S/cm.[11,12]

One of the most successful applications of sol-gel encapsulation is in combination with ionic liquids. Vioux et al. showed that sol-gel encapsulated ionic liquids (ionogels) couple the unique properties of ionic liquids, such as low-vapor pressure, ionic conductivity and high electrochemical stability, with the advantages of the solid phase.[13,14] Moreover, the flexibility of sol-gel chemistry enables one to control the amount of water in the synthesis, which is an extremely important consideration in lithium-ion batteries.[15] In recent years sol-gel derived ionogels have been applied in applications related to electrochemical energy storage,[16,17] drug delivery[18] and luminescence.[19,20,14]

In this report we use non-hydrolytic sol-gel chemistry to encapsulate a solution of lithium polysulfides. The resulting material is a solid that contains redox-active lithium polysulfides. This material offers the potential for improved LSB, especially in helping to contain and package polysulfide catholytes. At the same time, this work demonstrates that through precise control of sol-gel chemistry, a water-reactive liquid can be encapsulated and retain its ionic conductivity and redox activity.

For this synthesis, a water-free sol is required due to the reactivity of lithium polysulfides, which undergo vigorous reaction with water according to Eqn. 1:

$$Li_2S_n + 2\ H_2O \rightarrow 2\ LiOH + H_2S + S_{n-1} \qquad [1]$$

In order to retain active lithium polysulfide species in the final gel it is extremely important to minimize the amount of water that is in the sol during gelation. To this end, we used a non-hydrolytic sol created by the reaction of silicon tetrachloride ($SiCl_4$) and tertiary butanol (t-butanol). The nucleophilic substitution of t-butanol onto $SiCl_4$ (Fig. 1a) constitutes the initial step in the formation of the sol. Electron-donor effects from the alkyl radical tend to direct the alcoholysis reaction in Fig. 1a towards formation of silanol and t-butyl chloride (pathway 2).[21] However in reactions between $SiCl_4$ and t-butanol, both hydrogen chloride gas and t-butyl chloride are produced.[22] The reaction rate can be controlled by modifying the ratio of $SiCl_4$: t-butanol and/or by adding a co-solvent. Prior work has shown that the gelation time can be controlled by adjusting the amount of t-butanol.[23] For instance, Corriu et al. found that a 2:1 molar mixture of t-butanol : $SiCl_4$ gelled within three hours.[24]

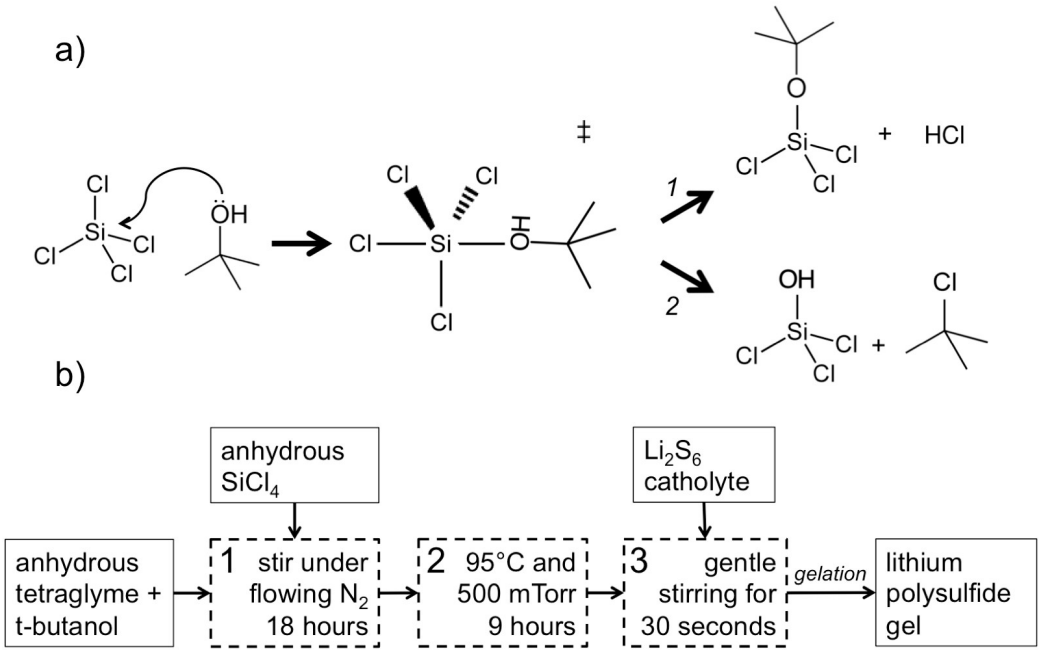

Fig. 1 (a) The alcoholysis reaction is the initial step in the non-hydrolytic sol-gel reaction between t-butanol and $SiCl_4$ and proceeds by two possible pathways. Pathway 2 produces hydroxyl groups which could later condense to form water. (b) Flow diagram of the PG synthesis. The two-step synthesis of water-free sol consists of mixing anhydrous reactants under nitrogen followed by heating the sol under vacuum. Finally the sol is mixed with Li_2S_6 catholyte to form the PG.

While the reaction in Fig. 1a does not include water as a starting material or solvent, water can still be generated via the condensation of hydroxyl groups created by pathway 2. For this reason, we fine-tuned the gelation time of the sol in order to generate a stable sol which was then heated under vacuum to remove as much water as possible. The result is a two-step synthesis for producing a water-free sol (Fig. 1b). In the first step anhydrous $SiCl_4$, tetraglyme (TG) and t-butanol are reacted under flowing nitrogen. In the second step, the sol is heated under vacuum to remove any volatile reaction products, but without inducing gelation. Finally, in the third step gelation is induced by mixing the sol with lithium polysulfide solutions.

Results and Discussion

The gelation times observed for various sol compositions (Table 1) are generally consistent with those reported by Corriu.[24] Gelation time increased as the molar ratio of $SiCl_4$: t-butanol was increased. The sol containing 1.49 moles of t-butanol remained liquid after over a day of observation. This sol composition was used for all of the PG experiments and is hereafter referred to simply as "sol".

Table 1 Gelation Times for Sols of Varying Composition

moles $SiCl_4$	moles TG	moles t-butanol	gelation time
		1.49	> 1 day
1	0.43	1.74	1 hour
		1.92	45 minutes

When lithium polysulfide was added directly to the sol, the mixture turned yellow and remained liquid for several months. The yellow color is attributed to sulfur that was produced via reaction with water in the sol according to Eqn. 1. Thus we introduced a drying step (Fig. 1b, step 2) where heat and vacuum were applied to the sol to remove any byproducts, especially water, which would have a deleterious effect on the battery.[15] After nine hours at 95°C and 500 mTorr we obtained a sol that, when combined with lithium polysulfide, formed a blood-red gel without any evidence of sulfur precipitation (Fig. S1a, ESI†).

The Fourier transform infrared (FTIR) spectrum of the sol (Fig. 2a) shows peaks for Si-O (1100 cm^{-1}) and O-H (3300 cm^{-1}).[25] In addition there are peaks at 1365, 1392 and 2967 cm^{-1} that are characteristic of C-H bonds on the butyl group. Because t-butyl chloride is quite volatile (P_{vap} = 34.9 kPa at 20°C) it is not likely to remain in the sol after nine hours of heat and vacuum. This provides convincing evidence that the nucleophilic substitution of t-butanol on $SiCl_4$ (Fig. 1) proceeds by pathway 1. The presence of the O-H peak confirms that pathway 2 also occurs and suggests that some water will be produced during the gelation reaction, but evidently this is not enough water to produce a macroscopic color change in the PG. After gelation the PG retains its characteristic electrochemical properties (*vide infra*).

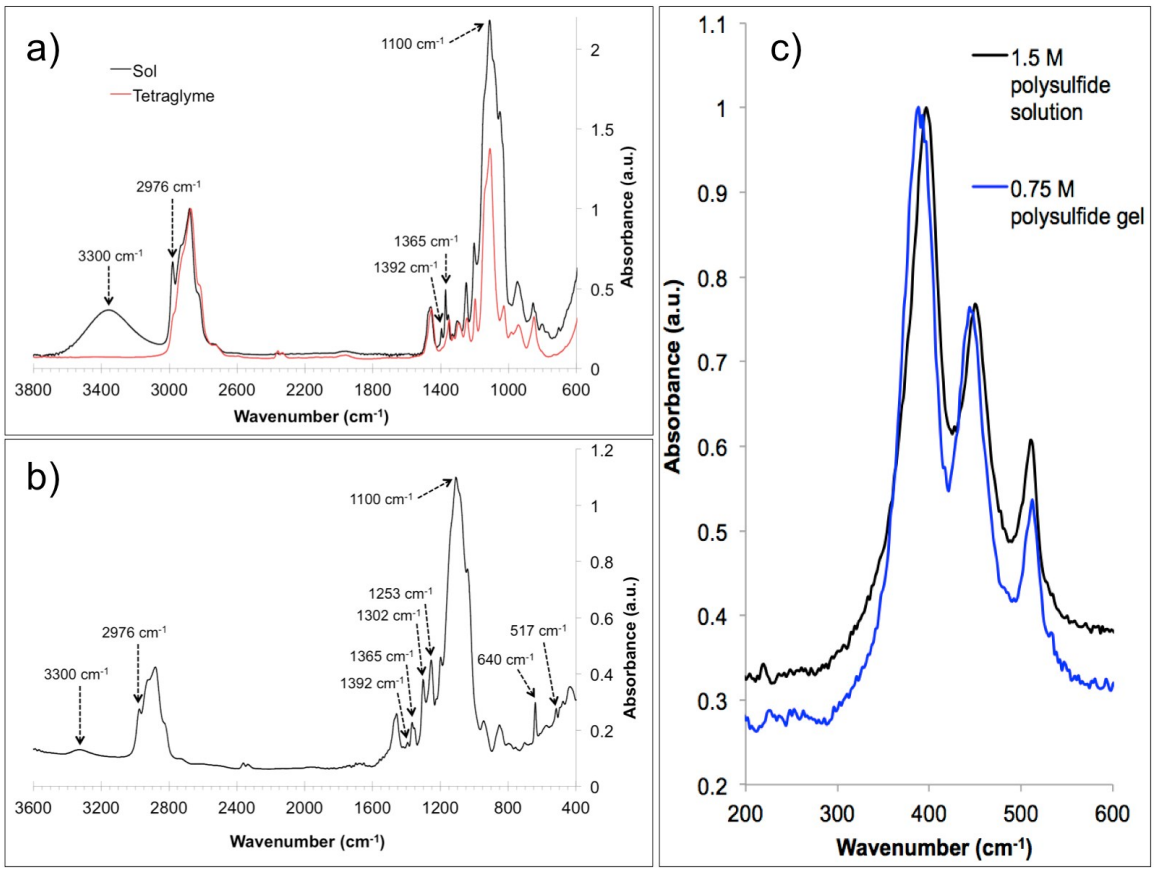

Fig. 2 Infrared spectroscopy of PG. (a) FTIR spectra of the sol after 9 hrs at 95°C and 500 mtorr. Both hydroxyl (3300 cm^{-1}) and t-butyl (2976, 1365, 1392 cm^{-1}) groups are present. (b) FTIR spectrum for the polysulfide gel prepared from 1:1 volume ratio of sol and 0.5 M Li_2S_6, 0.8 M $LiSO_3CF_3$ catholyte. The peaks are identified in Table 3. (c) Raman spectra for a 1.5 M Li_2S_6 solution and a 0.75 M Li_2S_6 gel, normalized to the peak near 393 cm^{-1}. A similar triplet of peaks is seen for both samples, indicating that the lithium polysulfide species are present in the PG.

Gelation of the sol/polysulfide mixture is caused by the lithium polysulfides and not by any other component of the mixture. A 1:1 volume mixture of sol : 0.8 M $LiSO_3CF_3$ electrolyte remained liquid after several months. Furthermore, 1:1 mixtures of sol : Li_2S_6 solution that did not contain $LiSO_3CF_3$ also gelled. As seen in Table 2, the gelation time was affected by the sol : catholyte volume ratio. The 1.5 M Li_2S_6 catholyte was too viscous to accurately pipette, so 0.5 M Li_2S_6 catholyte was used instead. For the 0.5 M Li_2S_6, decreasing the sol : catholyte volume ratio decreased the gelation time. One hour was an experimentally useful gelation time because it allowed us to perform electrochemical impedance spectroscopy (EIS) before the system gelled. Higher capacities are expected to result from gels with a higher concentration of sulfur, provided that higher viscosities do not lead to kinetic limitations.

Table 2 Gelation Behavior of Dehydrated Sol Mixed with Li_2S_6 Catholyte

sol : catholyte (by volume)	concentration Li_2S_6 in catholyte (M)	gelation time
2 : 1	1.5	2 hours
1 : 1	0.5	1 hour
1 : 2	0.5	20 minutes

The FTIR spectrum for the complete 1:1 PG is shown in Fig. 2b. The spectrum is similar to that of the as-prepared sol, with the addition of peaks associated with the SO_3CF_3 anion at 640, 1253 and 1302 cm^{-1}.[26,27] These peaks were identified by measuring the FTIR spectra of all the individual components of the catholyte solution (Fig. S3, ESI†). The FTIR peak positions for the PG are summarized in Table 3. The only potential evidence in the FTIR data for polysulfide species in the gel is a small peak at 517 cm^{-1} (Fig. S4, ESI†), but this is inconclusive. Based on the thorough spectroscopic study performed by Clark et al., we expect only this one weak absorbance for polysulfide species in the IR region.[28]

Table 3 Identification of FTIR Peaks for Polysulfide Gel

Band	Wavenumber (cm^{-1})	Assignment	Ref.
symmetric bend SO_3	640	LiTf	26
symmetric stretch CF_3	1228	LiTf	27
asymmetric stretch SO_3	1253, 1302	ion pairs (LiTf), $LiTf_2^-$, $LifTf_3^{2-}$	27
asymmetric stretch SiO	1100	SiO_2	25
bend C-H	1365, 1392	t-butyl	
stretch C-H	2976	t-butyl	
stretch O-H	3300	SiOH	

note: Tf = $SO_3CF_3^-$

Raman spectroscopy was far more effective than FTIR in confirming the presence of lithium polysulfides in the gel. Polysulfide species have a triplet of strong Raman scattering signals between 350 and 550 cm^{-1}.[28] Also the Raman spectrum is simplified because Si-O bonds are not Raman active. The Raman spectrum was further simplified by using a solution of Li_2S_6 without any $LiSO_3CF_3$ electrolyte as a control. In addition, THF was used as the solvent to lower the viscosity of the polysulfide solution and increase the solubility of Li_2S_6. Fig. 2c shows the Raman spectra obtained from a solution 1.5 M Li_2S_6 in THF and a PG made by combining dehydrated silica sol with the 1.5 M Li_2S_6 solution in a 1:1 volume ratio. In both the polysulfide solution and the PG we observe a triplet of peaks (393, 447 and 511 cm^{-1}) that is similar to that observed by Clark (384, 439 and 518 cm^{-1}) for solutions of Na_2S_4 in dimethylformamide.[28] The

peak position and shape are essentially unchanged after gelation, indicating that the polysulfide species are largely unaffected by the encapsulation process.

By dissolving away the polysulfide phase in THF, we were able to characterize the morphology of the mesoporous silica framework resulting from the sol-gel process. The use of non-polar solvents at the end of the solvent exchange process ensures that the solvent volatilizes without generating capillary forces which collapse the silicate network.[29] After solvent exchanging the PG, a pale pink monolith remained (Fig. S1b, ESI†) and nitrogen gas adsorption results (Fig. S2, ESI†) of this monolith indicated that the polysulfide species are effectively confined in an interconnected mesoporous network having high surface area and fine pore size. The silica component of the 2:1 PG had a BET surface area of 520 m^2/g, BJH pore volume of 0.254 cm^3/g and an average pore diameter of 1.96 nm. Considering that the as-prepared polysulfide had an average composition of Li_2S_6 and that the S-S bond length is 2.05 Å, the pores in the 2:1 PG are on the same size scale as the polysulfide chains.[30] The BJH pore distribution (Fig. 3a) shows that the majority of the pore area is attributed to pores that are less than 5 nm in diameter.

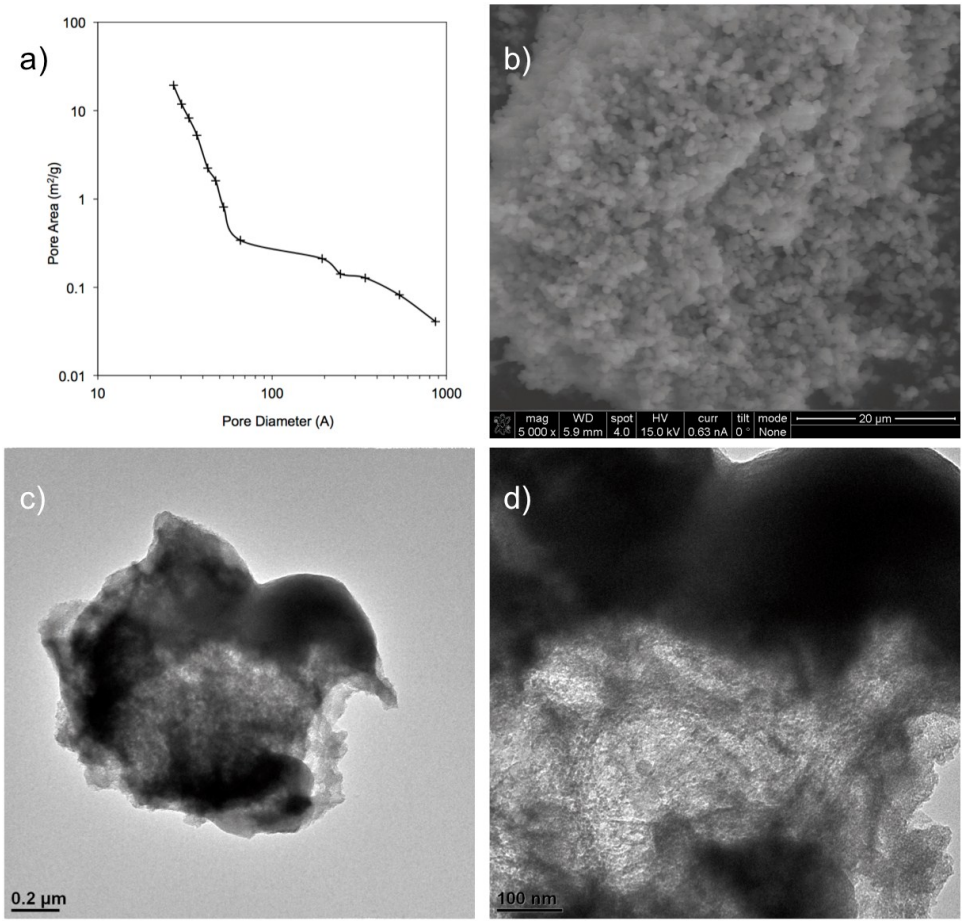

Fig. 3 (a) Pore size distribution obtained from BJH desorption data (b) SEM image of silica matrix that remains after the polysulfides are removed (c and d) TEM images of the silica matrix reveal a porous, non-crystalline structure.

The silica matrix was further characterized using electron microscopy. SEM (Fig. 3b) reveals that the gel is composed of primary particles that are around 1 μm in diameter. EDS analysis of this same frame shows that the sample contains 41.5 atomic % C, 37.8% O, 18.9% Si and trace amounts of F and S. The carbon is likely an impurity remaining from the solvent exchange process. The 2:1 atomic ratio of Si:O along with the small (0.37%) amount of S suggest that the matrix is pure silica and does not contain any S-O bonds. The same particles viewed under TEM (Fig. 3c, d) display a porous and non-crystalline structure that is consistent with the results of nitrogen adsorption.

The electrochemical properties of the PG were evaluated using cyclic voltammetry (CV), galvanostatic testing (GV) and electrochemical impedance spectroscopy (EIS). In an early work on lithium polysulfide electrochemistry, Yamin et al. reported a lithium metal/liquid polysulfide battery that displayed three distinct peaks in its CV while discharging and one peak during charging.[31] The three discharge peaks are all associated with the reduction of sulfur, i.e. breaking longer polysulfide chains into progressively shorter ones by adding lithium. In our CV experiment (Fig. S6, ESI†), at a sweep rate of 5 mV/s we observed only a single, broad reduction peak. The peak-to-peak separation for the PG is about 3 V, compared to only 1 V for the liquid polysulfide solution. The polarization seen for the PG is likely a result of the restricted motion of polysulfide species as well as the lower concentration of $LiSO_3CF_3$ electrolyte in the PG. CV at 5 mV/s is equivalent to one cycle in about 20 minutes. Evidently this sweep rate is too fast for the PG to respond.

The same electrochemical cell was used to monitor the impedance of the sol/catholyte mixture in-situ before and after gelation and cycling. The shape of the EIS data is a semicircle bounded by the real impedance axis. This shape is consistent with the equivalent circuit shown in ESI† Fig. S7, which consists of a capacitor with one resistor in series and one resistor in parallel. The first intercept on the real impedance axis is attributed to electrolyte resistance and the width of the semicircle represents the charge transfer resistance.[32] The EIS results are summarized in Table 4.

Before gelation, the electrolyte resistance of the cell is about 100 Ω, but after gelation this value doubles. This suggests that ion motion through the gel is somewhat restricted by the silica matrix. There is a modest rise in the charge-transfer resistance after gelation and then a decrease after cycling. The time constant of charge-transfer is calculated from the inverse of the frequency where the peak in the imaginary impedance occurs (Fig. 4b).[33] The time constant increases after gelation and cycling, though not dramatically. The increase could be due to the reaction of polysulfide species with the lithium electrode, creating insoluble polysulfides on the metal surface.

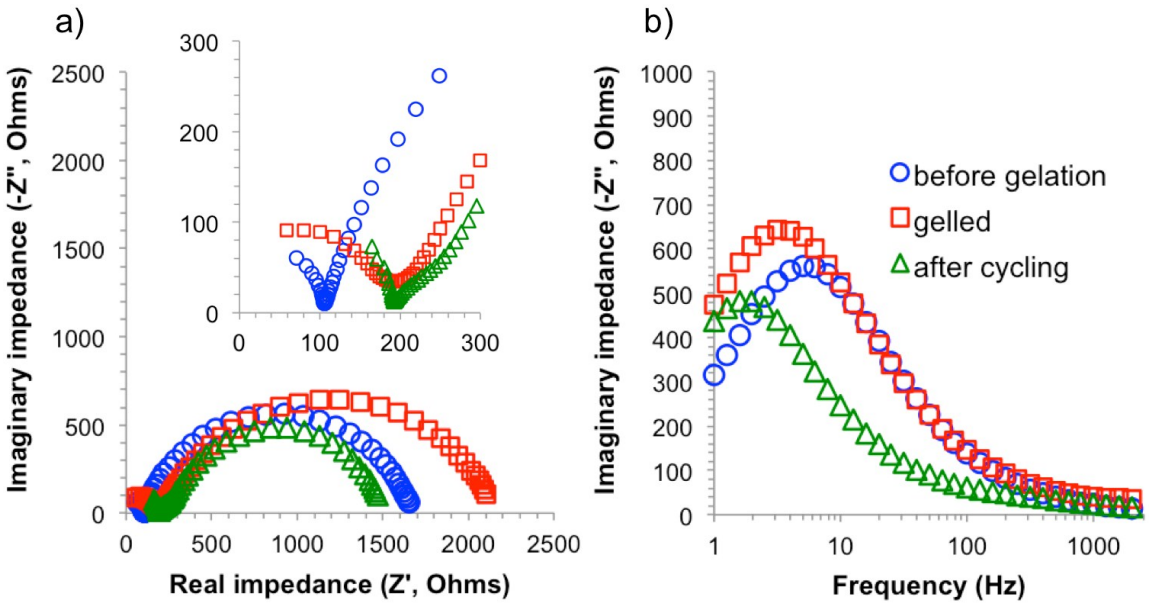

Fig. 4 (a) Nyquist representation of EIS data taken for the PG before gelation, after gelation and after cycling. The inset shows the high-frequency intercept of the real impedance axis. (b) The peak in the imaginary impedance *vs.* frequency corresponds to the time constant of charge-transfer in the PG.

Table 4 Summary of Impedance Data for Polysulfide Gel

Polysulfide cathode (state)	Open circuit potential (V)	Series resistance, R_s (Ω)	Charge-transfer resistance, R_{ct} (Ω)	Time constant, τ (ms)
Before cycling (sol)	2.29	103	1570	32
Before cycling (gel)	2.24	200	1960	50
After cycling (gel)	2.36	200	1300	88

GV experiments were performed (Fig. 5) by charging up to 2.8 V and discharging to 1.8 V (*vs.* Li^+/Li) with cycle times in the tens of hours. During GV experiments at 100 μA/cm^2 negligible (< 1% of theoretical) capacities were obtained. Overpotentials caused the voltage limits to be reached very quickly, indicating that the power of this cell is limited. However, using a current density of 50 μA/cm^2 (Fig. 5b) reasonable capacities were obtained. At this current, charging capacity was equal to about 62% of the theoretical reversible capacity, equivalent to 345 mAh/g sulfur. Discharge capacity was only about 26% of theoretical. The low Coulombic efficiency suggests that the shuttle mechanism is occurring in this cell; longer chain polysulfides are reacting at the lithium electrode, effectively creating an internal short. Nonetheless, the capacities are fairly stable over four cycles demonstrating the energy storage capability of the

PG. A single cycle at 10 μA/cm^2 (Fig 5a) showed better Coulombic efficiency of 84% and a lower charge voltage plateau at around 2.4 V (*vs*. Li$^+$/Li). The GV cycling data is summarized in ESI† Table S1.

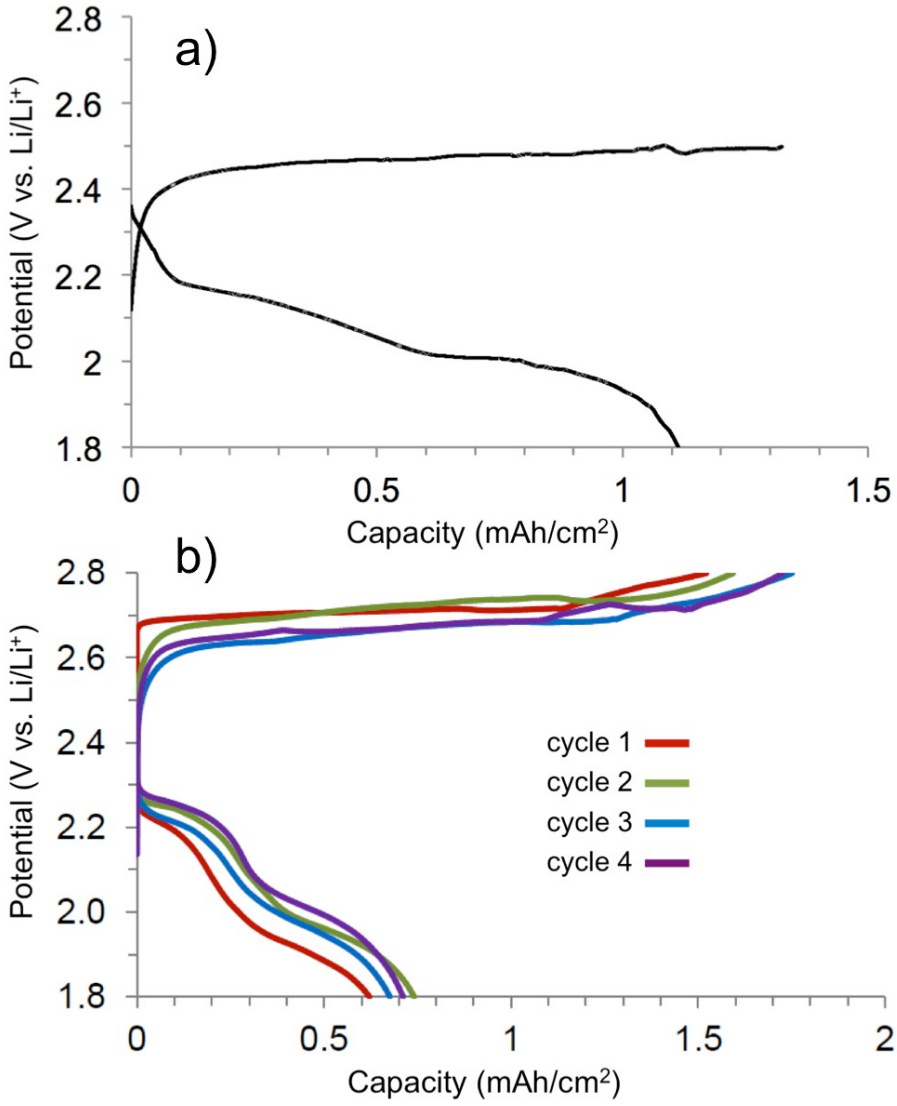

Fig. 5 Galvanostatic cycling data for a battery prepared from 1:1 volume mixture of dehydrated sol and catholyte (0.5 M Li_2S_6 and 0.8 M $LiSO_3CF_3$ in 30 : 70 :: TG : DXL). (a) One cycle at a current density of 10 μA/cm^2 (b) Four cycles are shown at 50 μA/cm^2.

The performance of this battery is promising given its remarkably simple construction. To form the complete cell, the PG is cast between a planar lithium anode and molybdenum current collector and forms a solid-state battery in-situ. After the PG solidifies there is no longer any problem of catholyte leakage. It should be possible to prepare solid LSB in small sizes and complex shapes by simply casting the PG around preformed metal electrodes.

There are several improvements that could be made on this initial proof-of-concept LSB. Having observed that $LiSO_3CF_3$ does not cause gelation, the power of the cells could be improved by increasing the concentration of $LiSO_3CF_3$ in the PG. Also, many contemporary studies on LSB make use of high surface area carbons as a means of increasing the conductivity at the cathode.[34,35,36,37] This could give significant power improvements over the flat molybdenum current collector used in these experiments. Finally, additives such as $LiNO_3$ will help to suppress the shuttle mechanism.[7,8] The inclusion of such additives in the PG should help to improve the Coulombic efficiency and discharge capacity of these batteries.

Conclusion

The synthesis employed in this work produces a water-free sol that successfully encapsulates water-sensitive lithium polysulfide. Nitrogen adsorption demonstrates that the silica framework is characterized by interconnected mesoporosity. Raman spectroscopy confirms that the polysulfides are largely unaffected by encapsulation. Electrochemical impedance spectroscopy reveals that there is only a minor change in the impedance properties of the polysulfide gel before and after gelation. Cyclic voltammetry and galvanostatic experiments indicate that the polysulfide gel displays the electrochemical features associated with liquid polysulfides and that even with the shuttle mechanism contributing to low coulombic efficiency, the cell was successfully charged and discharged at reasonable rates. The ability to form a solid gel material that contains electrochemically active lithium polysulfides represents a potentially new direction, especially for miniaturizing lithium-sulfur batteries.

Experimental

Materials

Lithium sulfide (Li_2S, 99.9%, Alfa Aesar), inhibitor-free anhydrous tetrahydrofuran (≥ 99.9%, Sigma-Aldrich) and anhydrous 1,3-dioxolane (99.8%, Sigma-Aldrich) were used as received. Sulfur (99.98%, Sigma-Aldrich), lithium triflate ($LiSO_3CF_3$, 99.995%, Sigma-Aldrich) and tetraethylene glycol dimethyl ether (tetraglyme, 99%, Sigma-Aldrich) were dried separately on a Schlenk line. After drying, tetraglyme was passed through a column of dry 4 Å molecular sieves in an argon-filled glovebox. Silicon tetrachloride ($SiCl_4$, 99.998%, Sigma-Aldrich) and anhydrous t-butanol (≥99.5%, Sigma-Aldrich) were used as received.

Catholyte preparation

The first step in the synthesis is to prepare a lithium polysulfide solution. Later this solution is mixed with the water-free sol to form the PG (Fig. 1b, step 3). A lithium polysulfide solution with an average composition of Li_2S_6 was prepared in an argon-filled glovebox using a method adapted from Rauh.[38] Tetrahydrofuran (THF) was added to Li_2S and sulfur powders in a molar ratio of 1 : 5 :: Li_2S : S and stirred for several hours. The powders reacted forming a blood-red solution. Tetraglyme (TG) was added and the resulting solution was stirred for one day at 55°C. The THF was then extracted from the solution by evaporating under vacuum at 85°C. Separately, electrolyte solution was prepared by adding $LiSO_3CF_3$ to dioxolane (DXL) and stirring for several hours. Once dissolved, the electrolyte solution was added to the Li_2S_6 solution. This combination of dissolved cathode material and electrolyte is referred to as a catholyte. Catholytes were made with two different polysulfide concentrations: 0.5 M and 1.5 M Li_2S_6 in TG : DXL

(30 : 70 by volume). These solutions contain 96 and 289 g/L of sulfur, for a maximum volumetric capacity of 161 and 484 Ah/L, respectively. Both catholytes contained 0.8 M $LiSO_3CF_3$ electrolyte.

Non-hydrolytic sol synthesis

To implement the sol processing scheme in Fig. 1b, the intial sol composition must be stable against gelation. Otherwise, the processing could not proceed to the evacuation step (Fig. 1b, step 2) where water and other volatile products are removed from the sol. A series of sols were prepared in order to determine the gelation time for the $SiCl_4$: TG : t-butanol system. The molar ratios of $SiCl_4$: TG : t-butanol were 1 : 0.43 : X where $1.49 < X < 1.92$. First, the t-butanol and TG were mixed together in a Schlenk flask in an argon-filled glovebox. The flask was fitted with a turnover septum stopper, removed from the glovebox and attached to high-purity nitrogen, which flowed through the flask and out through a bubbler containing 10 M aqueous potassium hydroxide. While stirring the t-butanol : TG mixture, $SiCl_4$ was added drop-wise over one minute and vapor was observed to condense on the walls of the flask (Fig. 1b, step 1). The sol containing 1.49 moles of t-butanol was found to be stable against spontaneous gelation for over a day. This sol composition was used to encapsulate the catholyte solution.

After 18 hours of mixing under flowing nitrogen, the flask containing the sol (1.49 moles t-butanol) was attached to a vacuum line equipped with a liquid nitrogen trap. The pressure was decreased to 500 mtorr and the sol was heated to 95°C over three hours (Fig. 1b, step 2). The sol bubbled initially as volatiles were removed, but eventually the bubbles ceased and the sol began to reflux. The sol was kept under these conditions for an additional six hours. The flask was then purged three times with nitrogen and moved into an argon-filled glove box with water concentration of 0.5 ppm. Opening the vial inside the glovebox had no effect on the measured water levels in the glovebox. Over the course of two months in the glovebox, the sol remained fluid with no evidence of gelation.

Sol-gel encapsulation of polysulfides

Sol-gel encapsulated polysulfides were prepared by mixing volume ratios of sol and polysulfide solution. Polysulfide solution was added to the sol and stirred gently for 30 seconds to mix the components (Fig. 1b, step 3). The mixture was then cast into electrochemical cells for testing and any remaining PG was saved for physical characterization.

Characterization of the polysulfide gels

Both FTIR and Raman spectroscopy were used to identify the constituents of the PG. After gelation and drying for two weeks, fragments of the PG were crushed, mixed with potassium bromide (KBr) and pressed into pellets in an argon-filled glovebox. The pellets were removed in argon-filled jars and quickly transferred into an FTIR chamber flooded with argon for FTIR analysis (Jasco FT/IR 670plus). Additionally, sodium chloride (NaCl) plates were used to obtain FTIR spectra of the liquid components of the PG, including the sol, catholytes, and $LiSO_3CF_3$ electrolyte. Again, the components were placed between the NaCl plates in the glovebox and transported to the FTIR chamber under argon. These spectra were used to help identify the peaks in the spectrum of the PG. Lithium polysulfides were identified in the gel using Raman

spectroscopy (Renishaw inVia Raman Microscope, 514 nm). Two samples were measured: a 1.5 M Li_2S_6 in THF solution and a 0.75 M PG, which were sealed under Ar in quartz cuvettes.

The microstructure of the sol-gel network was characterized by nitrogen gas adsorption analysis (Micromeritics ASAP 2010). In this case it was important to fully remove the polysulfide component without collapsing the silica network. These experiments were carried out with the 2 : 1 :: sol : catholyte PG and involved immersing the sample in a series of solvents. The initial immersion in THF is used to dissolve the polysulfide phase. Subsequent immersions are designed for solvent exchange with a series of solvents (DXL → acetone → pentane → cyclohexane) with decreasing polarity. Solvent exchange has been shown to be a good means of producing aerogels while maintaining the oxide structure.[Error! Bookmark not defined.] The nonpolarity of cyclohexane allows it to evaporate without collapsing the porous silica network. After solvent removal, the porous gel network was loaded into the sample tube for analysis.

Electrochemistry

Electrochemical measurements of the PG were carried out in 3-electrode cells that used a molybdenum working electrode, with a lithium counter electrode and lithium reference electrode (Fig. S5, ESI†). The area of the electrodes was 0.9 cm^2 and the distance between the working and counter electrodes was fixed at 1 mm using a polyethylene (PE) spacer. The cell contained approximately 90 µl of 0.25 M Li_2S_6 gel. This gives a theoretical capacity of 8.0 mAh/cm^2 for the full reduction of sulfur to Li_2S. However, because Li_2S_n species with $n < 3$ are insoluble, the sulfur should not be reduced beyond Li_2S_3 giving a theoretical capacity for reversible cycling of 2.7 mAh/cm^2.

The PG were characterized using cyclic voltammetry (CV) between 0.5 and 4.0 V (*vs*. Li^+/Li) at a sweep rate of 5 mV/s and galvanostatic cycling (GV) at current densites of 10, 50 and 100 $\mu A/cm^2$ with voltage limits of 1.8 and 2.8 V *vs*. Li^+/Li (Bio-logic SA VMP3 Multi-Channel Potentiostat). Electrochemical impedance spectroscopy (EIS) over the frequency range 10^5 to 10^{-1} Hz using a 10 mV signal was performed before and after gelation (Solartron 1252A Frequency Response Analyzer with Solartron SI 1287 Electrochemical Interface). Because gelation results in some shrinkage, the gel may detach from some portion of the electrodes resulting in anomalously high impedance. To overcome this problem, it is possible to re-establish contact by wetting the cell with the 0.8 M $LiSO_3CF_3$ electrolyte.

Acknowledgements

The authors greatly appreciate the support of the work by the Office of Naval Research.

References

1. J. B. Goodenough and Y. Kim, *Chem. of Mater.*, 2010, **22**, 587-603.
2. C. Barchasz, F. Molton, C. Duboc, J. C. Leprêtre, S. Patoux, and F, Alloin, *Anal. Chem.*, 2012, **84**, 3973-3980.
3. A. Manthiram, Y. Fu and Y. S. Su, *Acc. Chem. Res.,* 2013**, 46**, 1125-1134.
4. Y. Yang, G. Yu, J. J. Cha, H. Wu, M. Visgueritchian, Y. Yao, Z. Bao and Y. Cui, *ACS Nano.,* 2011, **5**, 9187-9193.

5. Y. Liu, L. Si, X. Zhou, X. Liu, Y. Xu, J. Bao and Z. Dai, *J. Mater. Chem. A*, 2014, **2**, 17735-17739.
6. S. Evers and L.F. Nazar, *Acc. Chem. Res.,* 2012, **46**, 9187-9193.
7. Y. Yang, G. Zheng and Y. Chi, *Energy Environ. Sci.,* 2013, **6**, 1552.
8. X. Liu, T. Murata, H. Yasuda and M. Yamachi, *GS News Technical Report,* 2003, 10-15.
9. R. Demir-Cakan, M. Morcrette, Gangulibabu, A. Guéguen, R. Dedryvère and J.-M. Tarascon, *Energy Environ. Sci.*, 2013, **6**, 176-182.
10. Z. Lin, Z. Liu, W. Fu, N. J. Dudney and C. Liang, *Angew. Chem. Int. Ed.,* 2013, **52**, 7460-7463.
10. P. W. Wu, S. R. Holm, A. T. Duong, B. Dunn and R. B. Kaner, *Chem. Mater.*, 1997, **9**, 1004-1011.
12. M. Opallo and J. Kukulka, *Electrochem. Commun*., 2000, **2**, 394-398.
13. M. A. Néouze, J. L. Bideau and A. Vioux, *Prog. Solid State Ch.,* 2005, **33**, 217-222.
14. K. Lunstroot, K. Driesen, P. Nockemann, C. Görller-Walrand, K. Binnemans, S. Bellayer, J.L. Bideau and A. Vioux, *Chem. Mater.,* 2006, **18**, 5711-5715.
15. D. Aurbach, *J. Power Sources,* 2000, **89**, 206-218.
16. J. L. Bideau, J. B. Ducros, P. Soudan and D. Guyomard, *Adv. Funct. Mater.*, 2011, **21**, 4073-4078.
16. S. A. M. Noor, P. M. Bayley, M. Forsynth and D. R. MacFarlane, *Electrochim. Acta.,* 2013, **91**, 219-226.
18. L. Viau, C. Tourné-Péteilh, J. M. Devoiselle and A. Vioux, *Chem. Commun.,* 2010, **46**, 228-230.
19. A. Kavanagh, R. Copperwhite, M. Oubaha, J. Owens, C. McDonagh, D. Diamond, and R. J. Byrne, *J. Mater. Chem.,* 2011, **21**, 8687-8693.
20. J. Zhang, Q. Zhang, F. Shi, S. Zhang, B. Qiao, L. Liu, Y. Ma and Y. Deng, *Chem. Phys. Letters.,* 2008, **461,** 229-234.
21. A. Vioux, *Chem. Mater.,* 1997, **9**, 2292-2299.
22. D. Ridge and M. J. Todd, *J. Chem. Soc.,* 1949, 2637-2640.
23. W. Gerrard and A. H. Woodhead, *J. Chem. Soc.,* 1951, 519-522.
24. R. J. P. Corriu, D. Leclercq, P. Lefèvre, P. H. Mutin and A. Vioux, *J. Non-Cryst. Solids,* 1992, **146**, 301-303.
25. A. Beganskienė, V. Sirutkaitis, M. Kurtinaitienė, R. Juškėnas and A. Kareiva, *Materials Science (Medziagotyra),* 2004, **10**, 287-290.
26. C. P. Rhodes and R. Frech, *Solid State Ion.,* 2000, **136-137**, 1131-1137.
27. A. G. Bishop, D. R. MacFarlane, D. McNaughton, and M. Forsyth, *J. Phys. Chem.,* 1996, **100**, 2237-2243.
28. R. J. H. Clark and D. G. Cobbold, *Inorg. Chem*., 1978, **17**, 3169-3174.
29. J. H. Harreld, W. Dong and B. Dunn, *Materials Research Bulletin*, 1998**, 33**, 561-567.
30. B. Meyer, *Chem. Rev.* 1976, **76**, 367-388.
31. H. Yamin, S. Gorenshtein, J. Penciner, Y. Sternberg and E. Peled, *J. Electrochem. Soc*. 1988, **135**, 1045-1048.
32. A. J. Bard, and L. R. Faulkner, *Electrochemical Methods Fundamentals and Applications*, 2001, ISBN: 0-471-04372-9.
33. S.-M. Park and J.-S. Yoo, *Anal. Chem.,* 2003**, 21,** 455A-461A.
34. G. Zheng, Y. Yang, J. J. Cha, S. S. Hong, and Y. Cui, *Nano Lett.* 2011, **11**, 4462-4467.

35. H. Wang, Y. Yang, Y. Liang, J. T. Robinson, Y. Li, A. Jackson, Y. Cui and H. Dai, *Nano Lett.* 2011, **11**, 2644-2647.
36. C. Liang and N. J. Dudney, J. Y. Howe, *Chem. Mater.* 2009**, 21**, 4724-4730.
37. X. Ji, K. T. Lee and L. F. Nazar, *Nat. Mater.* 2009, **8**, 500-506.
38. R. D. Rauh, F. S. Shuker, J. M. Marston and S. B. Brummer, *J. Inorg. Nucl. Chem.* 1997, **39**, 1761-1766.